Depth profiling of light elements using a nuclear microprobe

Terwagne, Guy; Bodart, Franz; Demortier, Guy

Published in:
Nuclear Instruments and Methods in Physics Research, Section B: Beam Interactions with Materials and Atoms

DOI:
10.1016/S0168-583X(99)00514-5

Publication date:
1999

Document Version
Early version, also known as pre-print

ELSEVIER

Nuclear Instruments and Methods in Physics Research B 158 (1999) 228–235

NIM B
Beam Interactions with Materials & Atoms

www.elsevier.nl/locate/nimb

Depth profiling of light elements using a nuclear microprobe

G. Terwagne *, F. Bodart, G. Demortier

Laboratoire d'Analyses par Réactions Nucléaires, Facultés Universitaires Notre-Dame de la Paix, rue de Bruxelles 61, B-5000 Namur, Belgium

Abstract

In this paper, we present some examples of depth profiling of light elements with a nuclear microprobe performed at LARN during the last decade. Some new possibilities of ion beam microanalysis of light elements with our 2 MV Tandetron accelerator are also discussed.

The first example of application consists of depth profiling of nitrogen and aluminium on a SiAl alloy implanted with nitrogen. The nuclear microprobe was used to determine three-dimensional distribution of aluminium, silicon and nitrogen in a specific grain of the implanted alloy. The nitrogen depth profile was measured using the well known $^{15}N(p,\alpha\gamma)^{12}C$ nuclear resonant reaction at 429 keV. The aluminium depth profile was measured with the resonant nuclear reaction $^{27}Al(p,\gamma)^{28}Si$ at 991.8 keV.

Depth profiling of carbon and oxygen is also possible using nuclear reactions induced by ^{3}He particles. Nuclear reactions like $^{12}C(^{3}He,p_i)^{14}N$ $(i = 0, 1, 2)$ or $^{16}O(^{3}He,\alpha_0)^{15}O$ were used to measure local wear tracks on a diamond coating after a fretting test against a Cr steel ball.

PIXE microprobe and nuclear reactions induced by deuterons were also used to characterise the gold–silicon alloy formed by the diffusion of silicon into gold foils. The nuclear reaction $^{28}Si(d,p)^{29}Si$ in a transmission geometry was used in order to depth profile silicon especially in the grain boundaries of the gold–silicon alloy.

Some new perspectives of depth profiling light elements are also presented using our new 2 MV Tandetron accelerator, such as high energy ^{4}He microbeams for depth profiling of carbon or nitrogen.

1. Introduction

Light elements such as carbon, nitrogen and oxygen play an important role in the surface treatment of steels, glasses or polymers. Protective, decorative or adhesive coatings on such substrates can be made by different techniques like Ion Implantation, DC-magnetron Sputtering, Ion Beam Assisted Deposition (IBAD) or Chemical Vapour Deposition (CVD). Quantitative analysis and depth profiling of light elements can be performed using Nuclear Reaction Analysis (NRA) induced by particles giving nuclear reactions with a positive Q-value, while Particle Induced X-ray Emission (PIXE) or Rutherford Backscattering Spectroscopy (RBS) are often not very convenient for light elements determination for substrates with $Z > 10$.

* Corresponding author. Tel.: +32-81-72-54-78; fax: +32-81-72-54-74; e-mail: guy.terwagne@fundp.ac.be

0168-583X/99/$ - see front matter
PII: S0168-583X(99)00514-5

An interesting review on the analysis of light elements by nuclear reaction analysis using microprobe was made at Shanghai conference in 1994 [1]. Only 8% of the papers of the five conferences concerning nuclear microprobes has been dedicated to light element analysis. The cross sections of nuclear reactions induced by deuterons or ^{3}He particles are often in the range of mbarns while the cross sections of RBS and PIXE are thousand times higher, which explains that those techniques are preferred to NRA, especially for microanalysis.

For example, microanalysis of coatings deposited on various substrates can be useful in order to study light elements in small tracks with dimension in the range 50–500 μm due to friction or wear test [2].

In this paper, we present some examples of depth profiling of light elements performed at LARN with the nuclear microprobe coupled to the 2.5 MV van de Graaff accelerator [2–4]. We will explain the advantage of combining different nuclear techniques in order to get more information and to obtain quantitative analysis of the specimen of interest. Some new perspectives with our new 2 MV Tandetron accelerator are also presented.

2. Nitrogen implanted into Si–Al alloy

2.1. Nitrogen implantation

The aluminium alloy "AS12UN" is a material used mainly in foundries due to its special ability of easily being cast. The major elements of this alloy are Al (84%), Si (12%), Cu (1%), Ni (1%) and Mg (1.15%) with some traces of Ti, Fe, Mn, Sn and Pb. The dilatation coefficient of this alloy is very low (1.95×10^{-5}/K) which makes it candidate for applications in automobile engines (e.g. pistons). The morphology of the alloy is composed of three phases: crystalline silicon grains included in the aluminium phase and an eutectic alloy. The size of the silicon grains depends on the cooling rate of the molten alloy. Typical grains of 150–200 μm in dimension have been observed in the aluminium phase. Fig. 1a shows a SEM micrograph of a selected silicon grain of the AS12UN alloy.

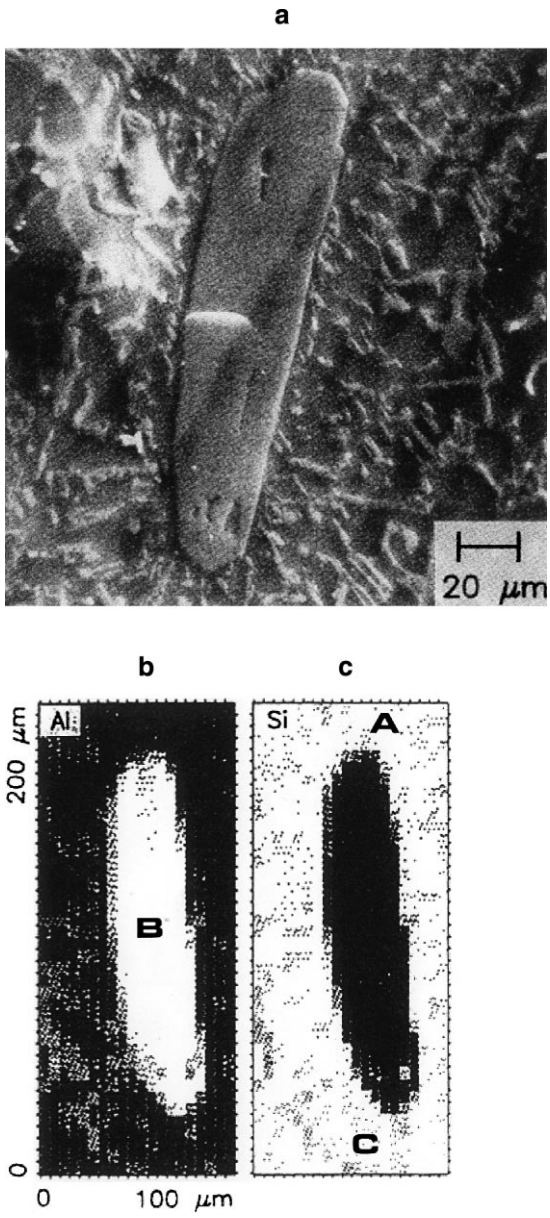

Fig. 1. (a) SEM micrograph of a selected silicon grain included in the "AS12UN" alloy. PIXE micro-beam map around the same silicon grain showing, respectively, (b) the aluminium and (c) the silicon concentrations.

Around the grain, we can observe the eutectic phase.

Tribological measurements have shown that the wear of this alloy is reduced by a factor of two

when nitrogen is implanted with doses ranging from 1×10^{17} to 5×10^{17} N^+/cm^2. Since it is known that nitrogen implantation in pure aluminium and in pure silicon leads to the formation of the corresponding nitrides [5], the challenge is to investigate the type of compounds appearing in the implantation process of the alloy and the behaviour of nitrogen after tribological experiments.

Prior to implantation, the surface of the sample was polished down to a grain size of 1 μm using different silicon carbide paper and diamond pastes. The sample was implanted with 100 keV $^{15}N_2^+$ for a dose of 5×10^{17} N^+/cm^2. The beam current density was 10 $\mu A/cm^2$ and the temperature of the specimen was kept lower than 30°C throughout the implantation procedure. The use of ^{15}N ions for implantation allowed us to profile nitrogen using the well known and very intense $^{15}N(p,\alpha\gamma)^{12}C$ resonant nuclear reaction which occurs at 429 keV [6,7].

2.2. Elemental analysis

All experiments were performed at the nuclear microprobe facilities of LARN. Combining PIXE and resonant nuclear reaction analysis (RNRA) techniques, we have measured all major elements present in and around a silicon inclusion in the specimen (Fig. 1a). A Si(Li) detector placed at 135° in the vertical plane with respect to the incident beam was used to precisely locate the silicon inclusions but, due to the strong absorption effects, accurate quantitative and depth measurements were difficult. Maps of aluminium and silicon using PIXE technique were obtained with a proton beam of 1 MeV focussed to 5 μm diameter. The pixel resolution was in the same range and the results are shown in Fig. 1b and c. We can easily observe a correlation between the maps and the SEM picture (Fig. 1a).

In order to obtain an aluminium depth profile in the same area, we have used the nuclear resonant reaction $^{27}Al(p,\gamma)^{28}Si$ which occurs at 991.8 keV [8]. The incident energy of protons varied step by step from 990 to 1007 keV. The γ-rays of 1778 keV emitted from the residual nucleus (^{28}Si) were detected in a 70% efficiency germanium detector placed at 135° in the horizontal plane with respect to the incident beam.

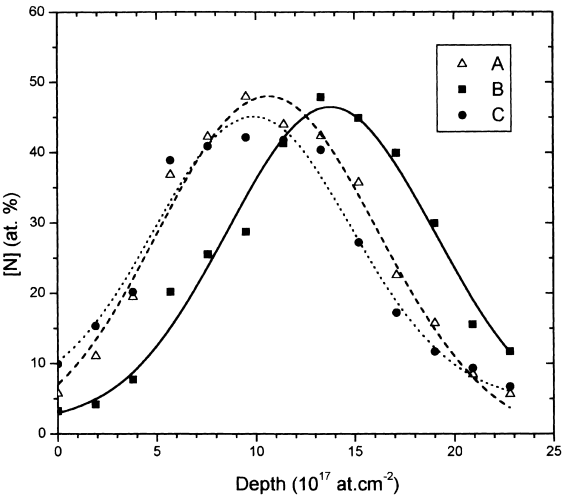

Fig. 2. Nitrogen depth distributions measured at three impacts positions shown in Figs. 1b and 1c. Impact points A and C are located outside the silicon grain while impact point B is inside the silicon grain. The lines connecting the data points were drawn to guide the eye.

Analysis of implanted nitrogen was made using the narrow ($\Gamma < 200$ eV) $^{15}N(p,\alpha\gamma)^{12}C$ nuclear resonant reaction which occurs at 429 keV. The nitrogen depth profile was obtained by varying the incident proton energy from 427 to 455 keV in steps of 2 keV and counting the prompt γ-rays of 4.43 MeV emitted by the ^{12}C residual nucleus. The detection geometry was the same as for aluminium depth profiling. Fig. 2 shows the nitrogen depth profile in the silicon grain (curve B) and outside the grain (curves A and C).

3. Analysis of transferred layer into wear tracks

3.1. Sample preparation

Diamond coatings of 5 μm in thickness were grown on WC-Co flat inserts (grade K10) with a hot filament chemical vapour deposition process [9]. The reactor was operated under a hydrogen methane mixture (50 mbar) with assistance of a W filament at about 2100°C. The substrate temperature during deposition was approximately 900°C. The coatings were then submitted to a low

amplitude oscillating sliding wear test. The 100Cr6 steel ball counter-body (10 mm diameter) was loaded with a dead weight of 4 N against the diamond coated flat. The diamond-coated sample was oscillated with a stroke of 100 μm and a frequency of 10 Hz for 100 000 cycles. Fig. 3 shows that a transferred layer has been formed after the fretting test on the diamond coating in the contact zone.

3.2. Transferred layer analysis

Quantitative analysis of carbon, oxygen and iron can be performed simultaneously by using nuclear reactions and RBS induced with ^{3}He particles. The cross-section of the nuclear reactions $^{12}C(^3He,p_i)^{14}N$ or $^{16}O(^3He,\alpha_0)^{15}O$ are sufficiently high for depth profiling of carbon and oxygen, even with a low current micro-beam (0.5 nA). For the analysis of oxygen, we have used the large resonance, which occurs at 2.392 MeV. At a detection angle of 90°, the differential cross section of this resonance is about 5 mb/sr. Carbon can also be analysed simultaneously using $^{12}C(^3He,p_1)^{14}N$ nuclear reaction. Protons were detected with a totally depleted annular surface barrier detector placed at a backward angle. The solid angle of this detector was 65 msr. The cross section of this reaction shows a maximum around 2.4 MeV [10]. The same detector was also used for RBS analysis of the high Z elements (Fe, Cr, ...) deposited as debris from the 100Cr6 steel ball counter-body. Fig. 4 shows RBS spectra observed in the annular detector at three different impact points on the track, for the same incident charge (0.1 μC). The thickness of the transferred layer are not homogeneous and we have split the signal due to iron into five different zones in order to depth profile

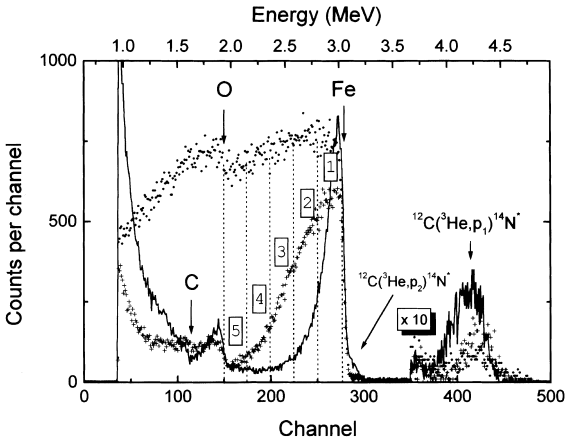

Fig. 4. RBS spectra recorded for the same incident charge (100 nC) at three different impact points on the track, showing three different thickness of the transferred layer. The full line spectrum corresponds to a dark zone; the spectrum represented by crosses was taken in a semi-bright zone, while the dot spectrum was recorded in a bright area of the specimen. The regions of interest labelled from 1 to 5 cover the information coming from iron and are named from Fe_1 to Fe_5 in Fig. 5.

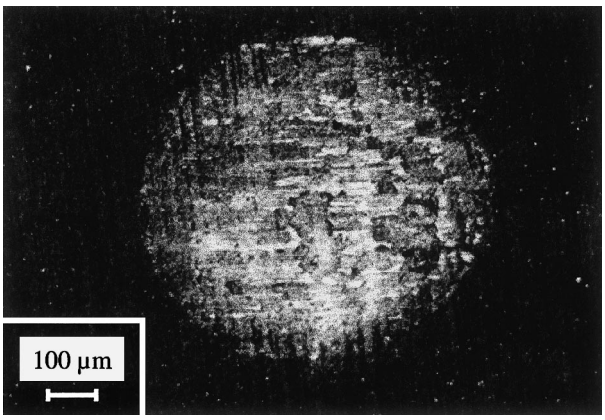

Fig. 3. Optical picture showing the track obtained on the diamond-coating layer after the fretting wear test. The length of the index is 100 μm and the estimated dimension of the wear track is about 500 μm.

the high Z elements present in the transferred layer. It should be noted that for all RBS spectra, carbon coming from the diamond coating can be measured using the $^{12}C(^3He,p_1)^{14}N$ nuclear reaction and it is clearly seen that more carbon is observed when the transfer layer is thin. There is also an interference between the $^{12}C(^3He,p_2)^{14}N$ nuclear reaction and the ^3He retrodiffused by iron but in first approximation this contribution can be neglected. We can remove this contribution for absolute measurements.

Line-scans were performed in the track shown in Fig. 3. To do this, we have introduced six regions of interest on the RBS spectrum: the five regions in the iron signal as explained above and the last one on the peak corresponding to the $^{12}C(^3He,p_1)^{14}N^*$ reaction, named C_{p1}. Fig. 5 presents two line-scans of 27 and 20 steps; each step corresponds to a displacement of 10 μm. They were realised, respectively, at 2.435 and 2.560 MeV in order to be sensitive to oxygen present at the surface (2.435 MeV) or in the bulk (2.560 MeV). The line-scans were normalised with the integrated charge and the results are presented in Fig. 5. The first energy was chosen just above the energy of the 2.392 MeV resonance of the $^{16}O(^3He,\alpha_0)^{15}O$ reaction and we can observe in Fig. 5 a correlation between the O_{NRA} and Fe_1 or Fe_2 information, while no correlation can be found between O_{NRA} and Fe_5. At higher incident energy (2.560 MeV), a correlation between O_{NRA} and Fe_3 or Fe_4 is evident but no correlation can be observed between O_{NRA} and Fe_1 or Fe_2. We can conclude that iron and oxygen are bound together and the stoichiometry can be measured by simulating the RBS spectrum obtained at one impact point as mentioned above. For both energies, we can observe an anti-correlation between O_{NRA} and C_{p1}, which indicates that most of the information of the C_{p1} peak is coming from the diamond coating.

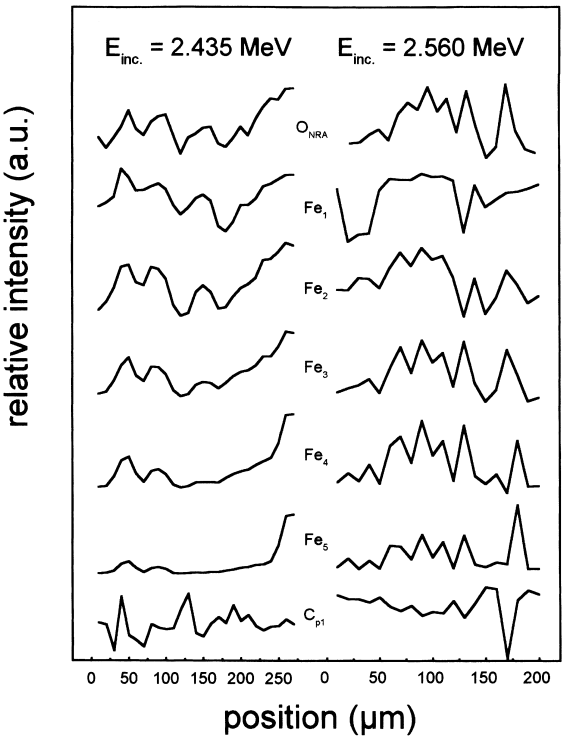

Fig. 5. Line-scans obtained at two different energies above the 2.392 MeV resonance of the $^{16}O(^3He,\alpha_0)^{15}O$ reaction. The O_{NRA} curves correspond to the region of interest on the $^{16}O(^3He,\alpha_0)^{15}O$ peak (Fig. 4), while O_{RBS}, Fe_i and C_{p1} curves were obtained from a region of interest which corresponds, respectively, to oxygen, iron and carbon from the $^{12}C(^3He,p_1)^{14}N$ reaction in the RBS spectrum (Fig. 4).

4. Eutectic Au–Si alloy in grain boundaries of gold

4.1. Samples preparation

Pure polycrystalline gold foils were rolled at room temperature down to thickness between 10 and 20 μm. A silicon film of 1 μm was then deposited on a part of the Au foil by using an electron gun evaporation technique. In order to obtain a good adhesion between gold and silicon, the temperature of the substrate was maintained to 400°C during evaporation. This temperature is slightly higher than the eutectic temperature (363°C) so that any Au–Si mixture at 400°C always contains a liquid phase. The liquid diffuses rapidly in the gold along well defined path: the gold grain boundaries. Silicon diffuses so rapidly that the eutectic Au–Si alloy is also observed at the rear of the gold film. Fig. 6 shows a SEM micrography of the eutectic Au–Si alloy along gold grain boundaries.

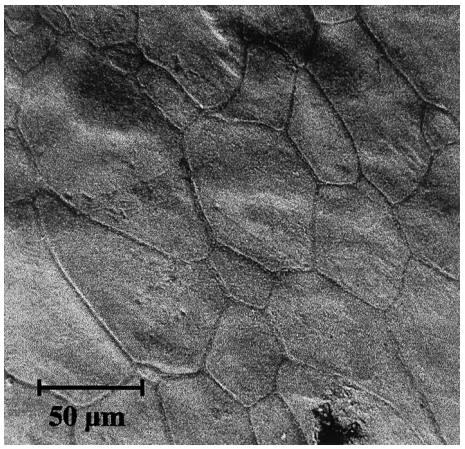

Fig. 6. SEM micrograph of the surface of a gold foil prepared for silicon diffusion. A liquid phase has been formed and has diffused throughout the whole sample thickness (12 μm).

4.2. Gold and silicon analysis

Combining nuclear reaction analysis (NRA) and particle-induced X-ray emission under deuteron irradiation (DIXE), it is possible to depth profile silicon along gold grain boundaries. The nuclear reaction $^{28}Si(d,p_0)^{29}Si$ is mainly governed by neutron capture involving no exchange of angular momentum ($l=0$). As a consequence, the maximum intensity in the proton emission is achieved in the forward direction. The cross section of this reaction at $E_d = 2.8$ MeV varies from 6 to 1 mb/sr when the angle of emission varies from 0° to 35° [11]. We therefore chose to detect the emitted protons in the forward direction. In this special arrangement, the solid angle of the particle detector (situated in the path of the incident beam) may be as high as 0.3 sr when the detector is placed very close to the sample. Incident deuterons pass through the Au–Si foil and nuclear reactions occur in the path of the incident beam. A second Au foil of 25 μm was placed behind the sample in order to completely stop the primary beam. We have estimated the detection limit for silicon around 0.5% due to the fact that the cross section of the nuclear reaction and the intensity of the incident deuterons beam (about 100–500 pA) are both relatively low.

As shown in Fig. 7 the quantitative determination of silicon at different depths below the surface is based on the comparison of the proton spectra obtained when pure silicon (75 μm) and gold–silicon samples are bombarded in the same geometrical arrangement. The p_0 peak was decomposed in seven slices, which correspond to seven different depths in the samples taking into account for the correction due to the stopping power. The results of the mapping for a scan of 35 by 80 μm are shown in Fig. 8a. The irradiation was made on the rear face of the Au–Si foil and it is clearly observed that silicon is mainly present in the gold grain boundaries. When the series of maps are corrected for the variation of the cross section of the nuclear $^{28}Si(d,p_0)^{29}Si$ reaction extracted from Fig. 7a, we obtain the silicon concentration maps of Fig. 8b. We can observe that the concentration of silicon is nearly constant (closed to that of the eutectic) along the full

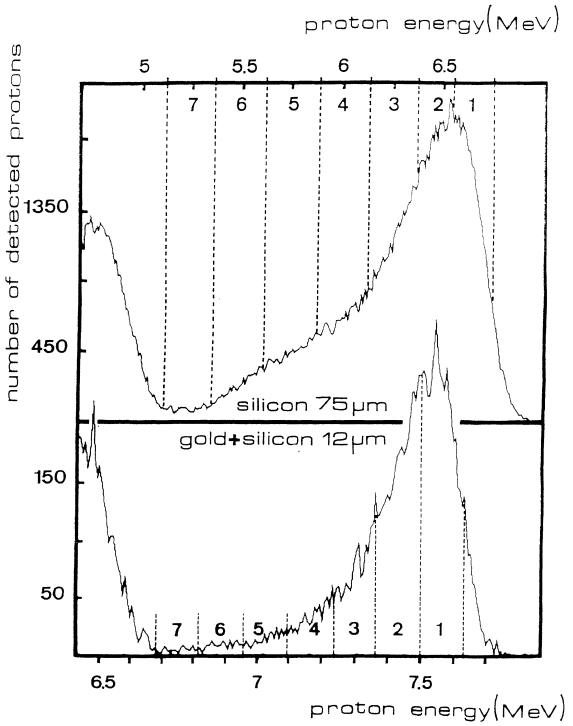

Fig. 7. Typical NRA spectra of the p_0 proton groups induced by 2.8 MeV deuterons on (a) a 75 μm thick pure silicon sample and (b) on a 12 μm thick gold foil prepared by silicon diffusion. The p_0 peak was divided in seven regions related to seven depth layers below the irradiated surface.

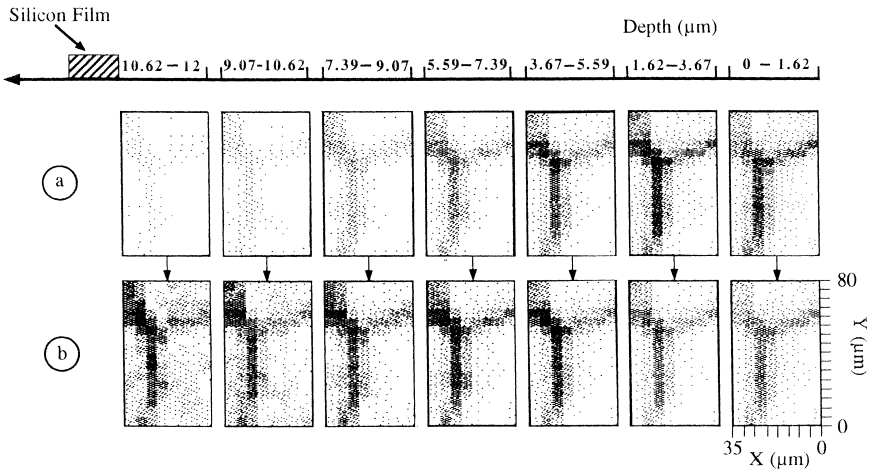

Fig. 8. Silicon profile maps in the whole thickness of a 12 μm thick gold foil divided in seven layers as defined in Fig.7. Proton intensities from each layer and (a) and corrected silicon concentrations obtained by using the data of Fig.7a.

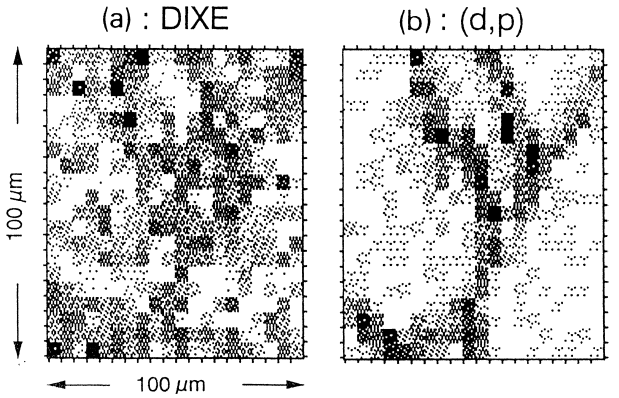

Fig. 9. X-ray and proton maps simultaneously obtained by scanning a region of 100×100 μm with a deuteron beam (3 μm in diameter) on the rear face of a 12 μm gold foil treated for Si diffusion during 1 h. The depth analysed for the DIXE scan (a) is around 0.5 μm while the depth analysed with the (d,p) reaction (b) is about 12 μm.

thickness into the grain boundary (nearly perpendicular to the surface of the foil).

A typical concentration map of Si obtained by DIXE in the grain boundaries at the backside of a 12 μm gold foil prepared for silicon diffusion is shown in Fig. 9a. The analysed depth of silicon and gold by DIXE involving the detection of K lines of Si and M lines of gold is much less than 1 μm below the surface. The analysed depth is mainly limited by the absorption of useful lines of silicon and gold and not by the deuteron range in the sample. We have compared the DIXE map with the map obtained by $^{28}Si(d,p_0)^{29}Si$ nuclear reaction (Fig. 9b). A correlation between the two maps can be observed but the spatial resolution of the NRA map is better than the spatial resolution of the DIXE map due to the fact that the information protons detected from the (d,p) reaction are produced along the whole thickness of the gold foil, which is about 12 μm.

5. New perspectives with a 2 MV Tandetron machine

Our new 2 MV Tandetron accelerator will be very useful because the maximum energy of this

HV machine depends on the charge states of the accelerated particles. New reactions often used in conventional nuclear techniques will be applied for the microbeam facilities at LARN.

In order to analyse up to micron depths and to profile simultaneously heavy and light elements, energetic ($E_\alpha > 5$ MeV) alpha backscattering analysis can be used. Nevertheless such a technique requires accurate measured values of the cross sections for ^{4}He scattering of the light elements. An interesting review of the experimental cross section data currently available for large angle scattering by the light elements ($4 < Z < 20$) were published by Leavitt et al. [12].

6. Conclusions

Quantitative microbeam analysis of light elements like C and O is possible even with a 5×3 μm ^{3}He beam of 0.5 nA in intensity. Some examples have shown that by combining different nuclear techniques like RBS, NRA, DIXE or RNRA, it is also possible to find out correlation between light elements. Carbon and oxygen can also be measured simultaneously using two different detectors. When the cross sections are known, it is possible to obtain quantitative concentrations for the light elements. Some new perspectives of nuclear reactions induced by a 2 MV Tandetron accelerator show that nuclear reaction analysis with a very small beam has also their place.

References

[1] G. Demortier, Nucl. Instr. and Meth. B 104 (1995) 244.
[2] G. Terwagne, F. Bodart, B. Blanpain, H. Mohrbacker, J.-P. Celis, Nucl. Instr. and Meth. B 104 (1995) 266.
[3] S. Lucas, G. Terwagne, F. Bodart, Proceedings of the International Conference on Application of Nuclear Techniques, Heraklio, Crete, Greece, 1990, p. 166.
[4] G. Demortier, S. Mathot, Nucl. Instr. and Meth. B 77 (1993) 312.
[5] S. Lucas, G. Terwagne, F. Bodart, Nucl. Instr. and Meth. B 50 (1990) 401.
[6] C. Rolfs, W. Rodney, Nucl. Phys. A 235 (1974) 450.
[7] G. Deconninck, G. Demortier, F. Bodart, Atomic Energy Rev. 2 (1981).
[8] K.M. Horn, W.A. Landford, Nucl. Instr. and Meth. B 34 (1988) 1.
[9] T. Leyendecker, O. Lemmer, A. Jürgens, S. Esser, J. Ebberink, in: Y. Tzeng, M. Yoshikawa, M. Murakawa, A. Feldman (Eds.), Applications of Diamond Films and Related Materials, Elsevier, Amsterdam, 1991, p. 105.
[10] G. Terwagne, Nucl. Instr. and Meth. B 122 (1997) 1.
[11] U. Strohbusch, W. Bakowsky, H. Lacek, Nucl. Phys. A 149 (1970) 605.
[12] J.A. Leavitt, L.C. McIntyre, Nucl. Instr. and Meth. B 56/57 (1991) 734.